

Power Handling and Polarization Maintaining of Photonic Wire Bonds

Peng Yao^{*a}, Matthew Konkola^a, Venkatesh Deenadayalan^c, Chad Newkirk^a, Yash Kabra^b, Md Omar Faruk Rasel^b, Mario Ciminelli^c, Stefan Preble^c, Dennis W. Prather^{ab}

^aPhase Sensitive Innovations Inc., 116 Sandy Dr Newark, DE, USA 19713

^bDept. of ECE, University of Delaware, Newark, DE, USA 19716

^cDept. of EME, Rochester Institute of Technology, Rochester NY 14623

ABSTRACT

Photonic wire bonding (PWB) offers a significant simplification in the integration and packaging of photonic integrated circuits (PICs). This study experimentally investigates the optical power handling and polarization-maintaining properties of PWBs. Power tests were conducted over extended periods (~18 days) and at high continuous-wave (CW) power levels (~1 W) on a group of PWB samples, demonstrating excellent power handling and longevity. Additionally, the state of polarization of PWB samples was characterized and compared with direct bonds and standard fiber connectors. The impact of misalignment on light polarization was analyzed, leading to the conclusion that a circular-cross-section PWB preserves light polarization comparable to a fiber connection mating interface.

Keywords: Photonic wire bonding, photonic integrated circuit, packaging, power handling, polarization maintaining

1. INTRODUCTION

Photonic Wire Bonding (PWB) has emerged as a powerful tool for high-performance and scalable optical interconnects in photonic integrated circuits (PICs). Unlike traditional coupling methods that rely on labor-intensive active alignments, PWB, as a labor-free, passive alignment approach, utilizes three-dimensional, freeform polymer waveguides fabricated via two-photon polymerization to bridge photonic devices with unmatched precision and efficiency[1]. PWBs enable high-efficiency photonic packaging in many applications, including fiber-to-fiber[2], fiber-to-chip[3], [4], and chip-to-chip[5] couplings. Sub-dB insertion loss of PWB has been experimentally demonstrated[2], [5]. And due to its extreme adaptability to misalignment and mode mismatching, PWB truly enables heterogeneous integration where PWBs are used to bring light from a III-V laser chip to a SiP chip[6], or to form an external cavity laser by coupling between gain chips and external cavity chips made of various materials[7], [8], etc. Using PWBs, ~1 Tbit/s data transfer[9] rate and high density photonic tensor core[10] have been experimentally demonstrated. Without a doubt, PWB will find more and more applications in PIC research, development and manufacturing. Despite its promising advancements, certain key optical properties of PWB, including power handling capability and polarization maintaining (PM) properties, remain relatively unexplored. This paper presents long-term tests of PWBs at 100mW, demonstrating that properly cladded PWBs are reliable for medium-power operation. High-power testing demonstrated continuous operation for over 6 hrs at 800mW. Additionally, we examined the PM properties of PWBs by comparing and analyzing the polarization states of light between PWB samples, regular fiber connectors, and directly-bonded samples. Although PWBs lack inherent PM features, they can maintain light polarization comparable to regular PM fiber connectors, provided proper alignment is achieved and sharp bending of the polymer waveguides is avoided.

2. STUDY OF PWB POWER HANDLING

The power-handling PWB samples were prepared using two 1x8 VGAs, pre-aligned and positioned with an approximate 250 μ m gap. Each corresponding channel was then connected using a PWB. Initial tests were conducted on PWBs without cladding, resulting in inconsistent outcomes. Some channels failed at relatively high power levels (>23dBm) after two days of testing, while others failed at lower power levels (~20dBm) within tens of minutes. All failures occurred at the center of the PWB, where the polymer waveguide is thinnest. Considering the tight mode confinement caused by the significant index contrast between the PWB polymer and air, it was suspected that overheating in areas of highest field density led to the failures. To address this problem, another test sample was prepared with the same VGA and PWB configuration. However, this time, the PWBs were cladded with a low-index polymer after processing.

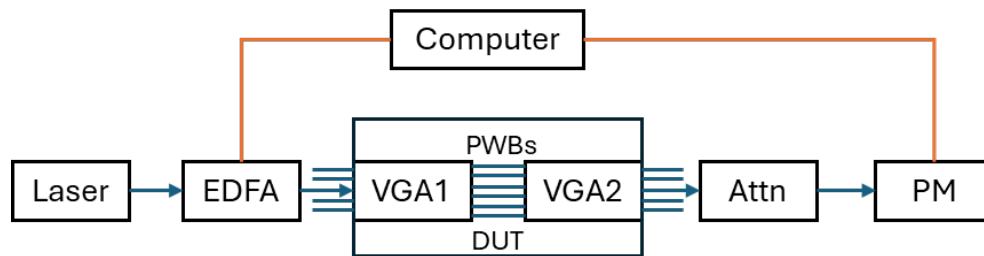


Figure 1. Block diagram of the PWB power test setup

Figure 1 shows the block diagram of the power-handling test setup. The input power level was controlled via direct commands to the EDFA module, and the EDFA output power was calibrated up to 2W before experiments. A fixed attenuator was placed between the DUT output and the power meter (PM) to ensure accurate measurements below the PM's saturation point. The PM output was recorded by a computer, and in the event of power loss or connection failure, the control software automatically shut off the EDFA.

Two experiments were conducted using the new PWB sample to evaluate both device longevity at medium power levels and its high-power handling capability. Figure 2 shows the recorded output power of the PWB sample over approximately 18 days of continuous testing. No degradation in insertion loss was observed, confirming the long-term reliability of PWB optical connections. Furthermore, the test channel remained undamaged after the extended tests.

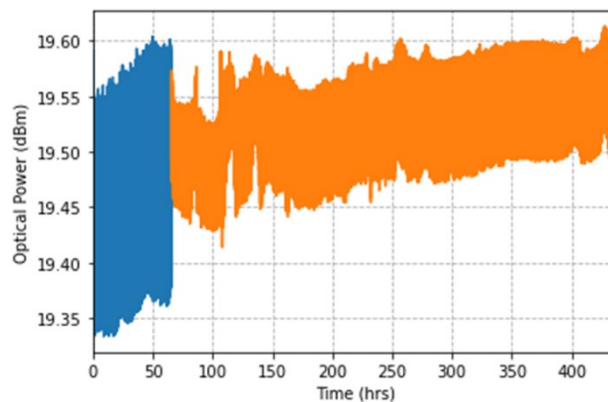


Figure 2. Long-term PWB study. The DUT output power is plotted over ~18 days. The blue and the orange data were interrupted briefly by resetting the laser output from constant current mode to constant power mode.

We continued our studies with higher optical input powers, ranging from 23dBm to 30dBm. At each power level, we continuously monitored the output power for at least six hours before progressing to the next level. The various DUTs successfully withstood testing at 23dBm, 27dBm, and 29dBm, but failed at 30dBm after varying durations. Figure 3(a), (b), and (c) present typical test results at 27dBm, 29dBm, and the outcome of a DUT that survived 30dBm input power. At power levels below 30dBm, the insertion loss was measured before and after each test, with no significant changes observed. The down-trend curves likely resulted from the gradual output power decrease of the EDFA—less than 1dB in all three cases—rather than an increase in PWB insertion loss. In contrast, the test at 30dBm exhibited a much larger power decrease, approximately 4dB over six hours. Further analysis confirmed that this increased loss was due to heightened PWB insertion, as evidenced by re-measuring the PWB insertion at a lower optical power level.

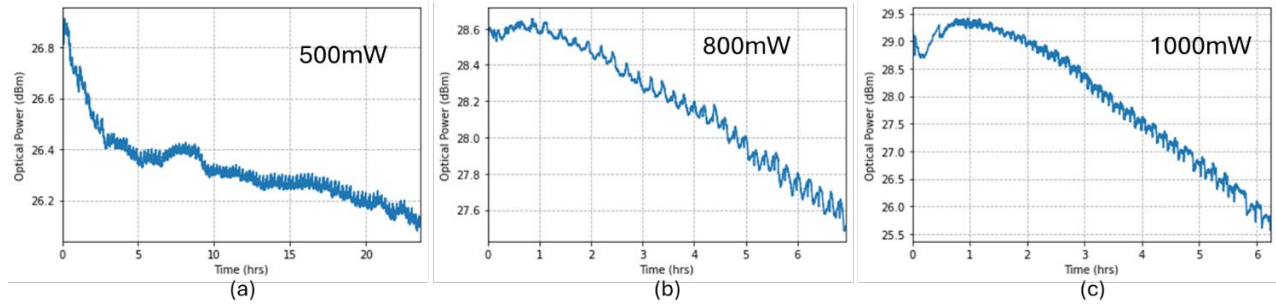


Figure 3 PWB power test results at different power levels. (a) 500mW input power. (b) 800mW input power. (c) 1W input power.

Compared to the power tests conducted with air cladding, the polymer-cladded PWB samples demonstrated significantly enhanced power handling capabilities. This improvement is attributed to an increase in mode size resulting from a reduced index contrast (from approximately 0.5 to 0.2) and improved thermal dissipation facilitated by the polymer cladding. Additionally, it is possible that the PWBs with air cladding experienced damage due to heat-induced stress. In contrast, the polymer cladding provides better mechanical support, reducing the likelihood of such stress-related damage.

3. STUDY OF PWB POLARIZATION MAINTAINING PROPERTIES

We prepared five assemblies for the PWB polarization-maintaining property study, as shown in Figure 4(a). Each assembly comprises two 1x8 VGAs. Each COTS VGA is equipped with 8 PM fibers, aligned with their slow axes in the VGA's horizontal direction. Four VGA pairs were integrated using the PWBs, as depicted in Figure 4(b) and (c). The VGAs were mounted on a substrate using a Ficontec® precision pick-and-place tool. This high-precision placement allowed us to precisely control the relative positioning of the two VGAs. To study the potential impacts of waveguide bending on PM properties, we deliberately introduced horizontal and vertical shifts during integration. The four samples were as follows: PWB1, with no intentional misalignment ($H=0\mu\text{m}$, $V=0\mu\text{m}$); PWB2, with a $20\mu\text{m}$ horizontal misalignment ($H=20\mu\text{m}$, $V=0\mu\text{m}$); PWB3, with a $10\mu\text{m}$ vertical misalignment ($H=0\mu\text{m}$, $V=10\mu\text{m}$); and PWB4, with a $20\mu\text{m}$ horizontal and $10\mu\text{m}$ vertical misalignment ($H=20\mu\text{m}$, $V=10\mu\text{m}$).

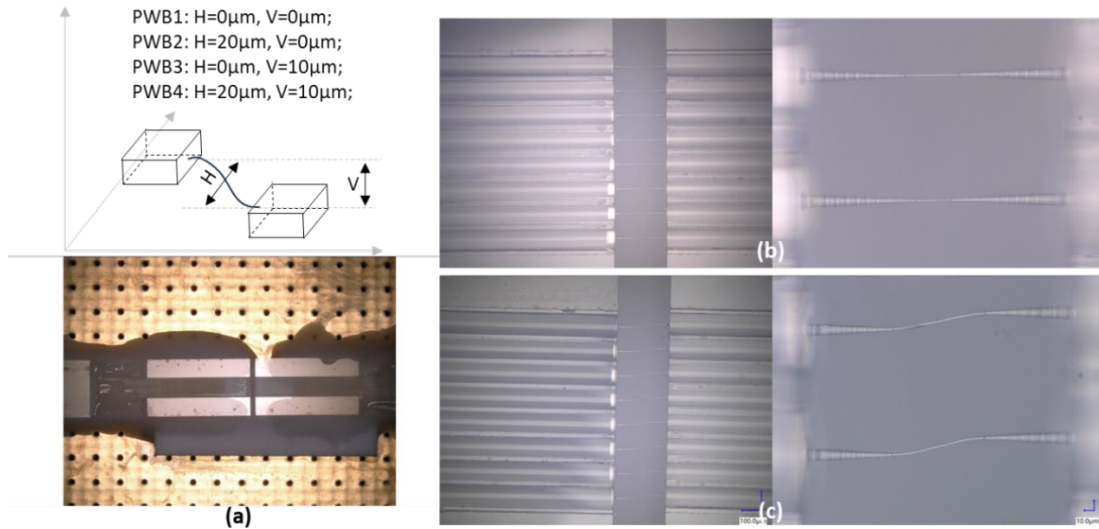


Figure 4. VGAs integrated by PWB. (a) Diagram of different VGA arrangements and an optical image of integrated VGAs on a carrier. (b) Optical images of PWBs with perfect alignment. (c) Optical images of PWBs with intentional horizontal misalignment ($H=20\mu\text{m}$, $V=0\mu\text{m}$).

We studied the light polarization states using a polarimeter setup, recording the output light polarization states over 5 minutes at 0.1-second intervals. The collected data was statistically analyzed to determine key polarization parameters such as ellipticity, azimuth angle, and the degree of linear polarization. Alongside the PWB samples, we prepared a similar 1x8 VGA assembly utilizing active alignment and direct epoxy bonding. Initially, the laser polarization states were tested as a reference, followed by tests on each channel of the direct bond sample and the PWB samples. Finally, a PM patchcord was inserted between the laser and the polarimeter to evaluate the output polarization states. Figure 5 illustrates all test configurations.

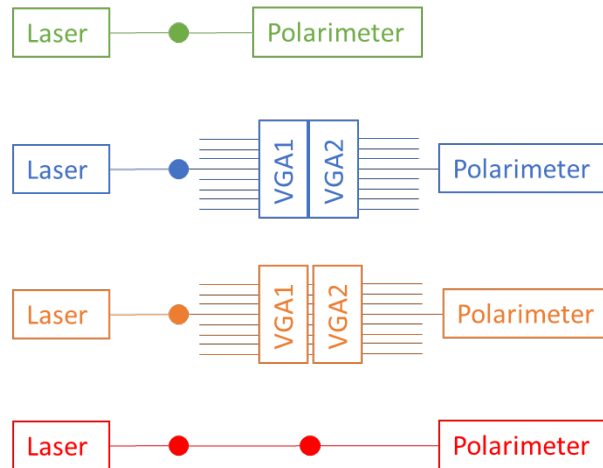


Figure 5. Polarimeter test configuration, Solid dots represent FC/APC fiber connections.

Figure 6 illustrates the comparison between insertion loss and the degree of linear polarization (DOLP) across all test channels. Due to fiber damage during shipping, four channels from the vertical offset sample (PWB3) and one channel from the diagonally offset sample (PWB4) were lost. In Figure 6, we present the time varying DOLP data in box whisker plots where a box is used to show the middle 50% of data between the first and third quartiles as well as “whiskers” extending to the minimum and maximum values. The results indicated that both DOLP average and fluctuation increased as alignment offsets were introduced in the PWBs. Without offsets, the PWB channels exhibited slightly poorer DOLP than the direct bond sample but outperformed a regular PM APC connector. As offsets increased, the PWB DOLP degraded, with some results falling below the patch cord reference. Vertical offsets had a more pronounced impact on DOLP compared to horizontal offsets for the TE polarized input. In Figure 6, channel insertion loss is plotted alongside the measured DOLP values. While a general trend of higher insertion loss with larger alignment offsets was observed, no definitive correlation between insertion loss and DOLP degradation could be established. Interestingly, the three channels with the highest insertion losses—PWB3-ch7, PWB4-ch1, and PWB4-ch2—still maintained DOLP values exceeding 90%. Similar observations were noted in the ellipticity data analysis, as shown in Figure 7.

Although PWBs with a circular cross-section lack inherent polarization-maintaining (PM) structures, they can still preserve light polarization due to their short length, yielding a performance comparable to standard PM fiber connectors. However, the PM properties of PWBs deteriorate significantly when waveguide bends are introduced to compensate for misalignment between coupling ports. Our observations showed greater degradation in the Degree of Linear Polarization (DOLP) and ellipticity in the vertically offset case, based on limited data points, compared to the diagonal offset case with the same vertical offset. This makes it difficult to establish a clear dependence of PM properties on the bending directions of PWBs. Nevertheless, all offset samples exhibited some degree of PM degradation compared to well-aligned cases. Additionally, individual fiber angle alignment within each VGA assembly contributed to PM degradation, though this effect was relatively minor, as inferred from directly bonded samples with similar alignment specifications. In summary, short, non-bending PWBs preserve light polarization on par with standard PM connectors, but their PM properties are highly influenced by the alignment of coupling ports.

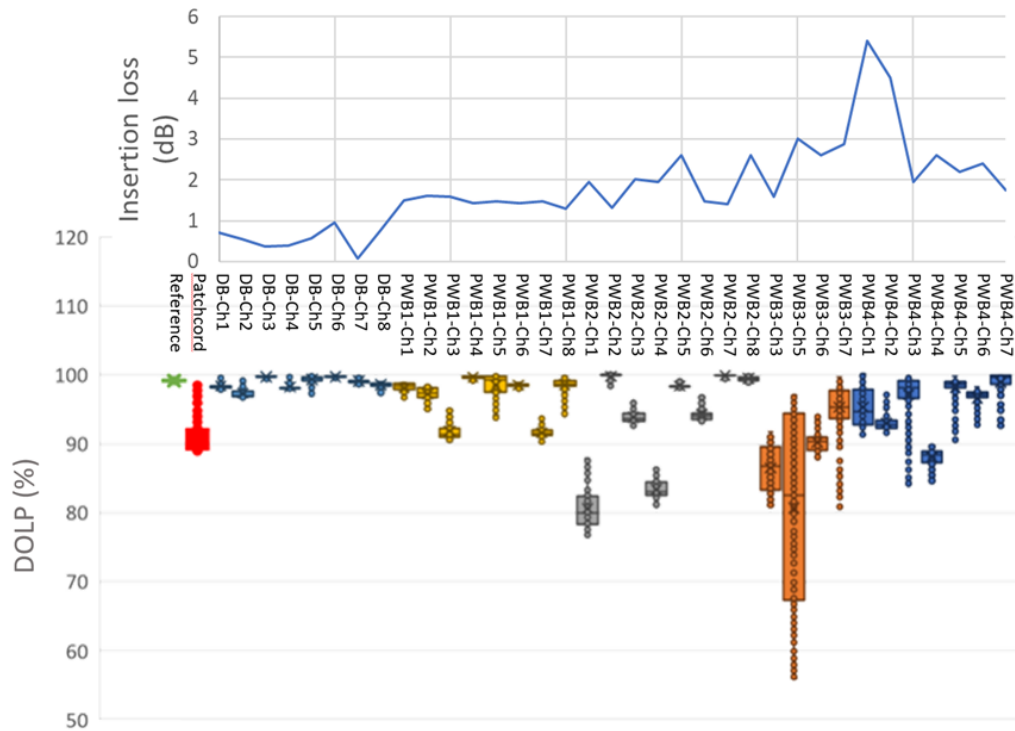


Figure 6. Comparison of insertion loss and degree of linear polarization. Measured DOLP of the laser (reference), the patchcord assembly, the direct bonded sample (DB), PWB with perfect alignment (PWB1), PWB with 20 μ m horizontal offset (PWB2), PWB with 10 μ m vertical offset (PWB3) and PWB with both horizontal and vertical offsets (PWB4).

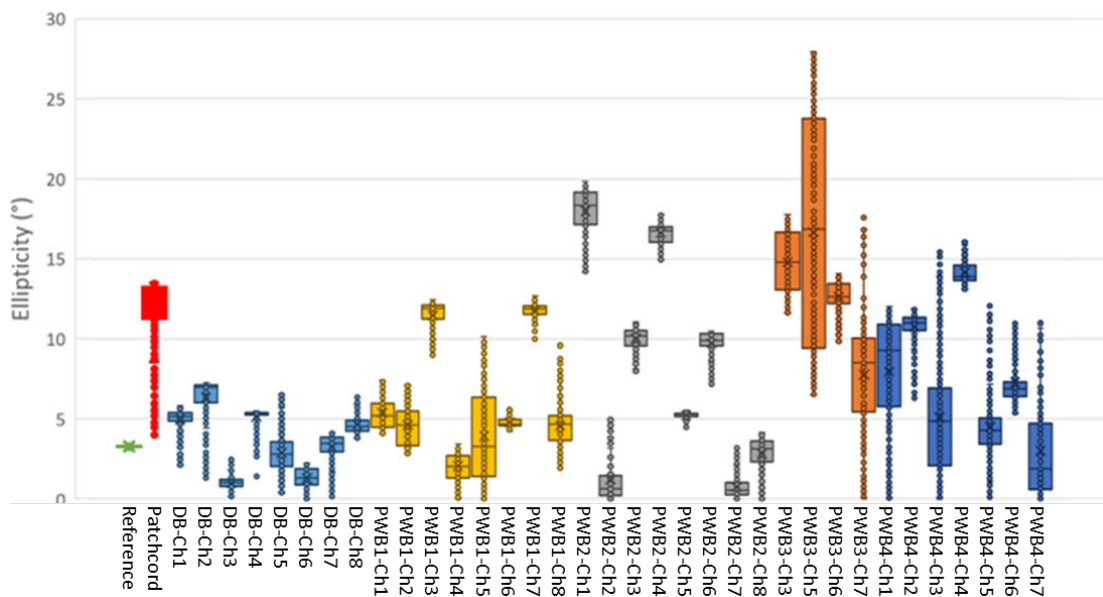


Figure 7. Measured ellipticities of the laser (reference), the patchcord assembly, the direct bonded sample (DB), PWB with perfect alignment (PWB1), PWB with 20 μ m horizontal offset (PWB2), PWB with 10 μ m vertical offset (PWB3) and PWB with both horizontal and vertical offsets (PWB4).

4. DISCUSSION

This paper presents an experimental study on the power handling and polarization-maintaining (PM) properties of photonic wire bonds (PWBs). Our findings indicate that PWBs with appropriate polymer cladding can reliably operate at medium power levels, such as 100mW, as demonstrated by an 18-day continuous test. Additionally, we showed that PWBs can sustain high power operation at 800mW for over six hours. However, further studies are required to assess longer testing durations and explore various PWB configurations.

We also examined the light polarization states after passing through PWB connections and compared these results with directly bonded cases and a PM patchcord. The results suggest that straight PWBs effectively preserve light polarization, while bends in PWBs significantly degrade PM properties, including the Degree of Linear Polarization (DOLP) and ellipticity. To enhance accuracy in measuring the impact of PWBs on light polarization states, future research should incorporate direct splicing in PM test setups to eliminate the influence of fiber connectors. Moreover, Polarization Extinction Ratio (PER) testing is recommended to better quantify PWB PM properties for practical system implementations.

REFERENCES

- [1] N. Lindenmann *et al.*, “Photonic wire bonding: a novel concept for chip-scale interconnects,” *Opt. Express*, vol. 20, no. 16, p. 17667, Jul. 2012, doi: 10.1364/OE.20.017667.
- [2] Y. Lei *et al.*, “In-Situ Multiphysical Metrology for Photonic Wire Bonding by Two Photon Polymerization,” Sep. 23, 2024, doi: 10.20944/preprints202409.1642.v1.
- [3] B. Lin, D. Witt, J. F. Young, and L. Chrostowski, “Cryogenic optical packaging using photonic wire bonds,” *APL Photonics*, vol. 8, no. 12, p. 126109, Dec. 2023, doi: 10.1063/5.0170974.
- [4] N. Lindenmann *et al.*, “Connecting Silicon Photonic Circuits to Multicore Fibers by Photonic Wire Bonding,” *J. Light. Technol.*, vol. 33, no. 4, pp. 755–760, Feb. 2015, doi: 10.1109/JLT.2014.2373051.
- [5] M. Blaicher *et al.*, “Hybrid multi-chip assembly of optical communication engines by in situ 3D nano-lithography,” *Light Sci. Appl.*, vol. 9, no. 1, p. 71, Apr. 2020, doi: 10.1038/s41377-020-0272-5.
- [6] M. R. Billah *et al.*, “Hybrid integration of silicon photonics circuits and InP lasers by photonic wire bonding,” *Optica*, vol. 5, no. 7, p. 876, Jul. 2018, doi: 10.1364/OPTICA.5.000876.
- [7] C. A. A. Franken *et al.*, “High-power and narrow-linewidth laser on thin-film lithium niobate enabled by photonic wire bonding,” Jul. 05, 2024, *arXiv*: arXiv:2407.00269. doi: 10.48550/arXiv.2407.00269.
- [8] Y. Xu *et al.*, “Hybrid external-cavity lasers (ECL) using photonic wire bonds as coupling elements,” *Sci. Rep.*, vol. 11, no. 1, p. 16426, Aug. 2021, doi: 10.1038/s41598-021-95981-w.
- [9] S. Juodkakis, “Laser polymerized photonic wire bonds approach 1 Tbit/s data rates,” *Light Sci. Appl.*, vol. 9, no. 1, pp. 72, s41377-020-0292–1, Apr. 2020, doi: 10.1038/s41377-020-0292-1.
- [10] E. Luan *et al.*, “Towards a high-density photonic tensor core enabled by intensity-modulated microrings and photonic wire bonding,” *Sci. Rep.*, vol. 13, no. 1, p. 1260, Jan. 2023, doi: 10.1038/s41598-023-27724-y.